Supplementary Information

A Lysosome-Specific Two-Photon Phosphorescent Binuclear Cyclometalated Platinum(II) Probe for *In Vivo* Imaging of Live Neuron

Yu-Man Ho,[a†] Ngan-Pan Bennett Au,[a,b†] Ka-Leung Wong,[c] Chris Tsz-Leung Chan,[d] Wai-Ming Kwok,[d] Ga-Lai Law,[d] Kwong-Kit Tang[e], Wai-Yeung Wong,[c] Chi-Him Eddie Ma,*[a,b] Michael Hon-Wah Lam*[a]

[a] Department of Biology & Chemistry, City University of Hong Kong, Tat Chee Ave., Kowloon, Hong Kong

[b] Centre for Biosystems, Neuroscience, and Nanotechnology, City University of Hong Kong, Tat Chee Avenue, Hong Kong

[c] Department of Chemistry, Hong Kong Baptist University, Waterloo Road, Kowloon, Hong Kong

[d] Department of Applied Biology & Chemical Technology, Hong Kong Polytechnic University, Hung Hom, Hong Kong

[e] LSD - HK Division, Leica Microsystems Ltd, Hong Kong

[†] Y.M.H. and B.N.P.A. contributed equally

* Corresponding authors:

Dr. Michael H. W. Lam
Department of Biology & Chemistry
City University of Hong Kong
Tat Chee Ave., Kowloon
Hong Kong SAR, China
Tel: (852)-3442-7329
Fax: (852)-3442-0522
Email: bhmhwlam@cityu.edu.hk

Dr. C. H. Eddie Ma
Department of Biology & Chemistry
City University of Hong Kong
Tat Chee Ave., Kowloon
Hong Kong SAR, China
Tel: (852)-3442-9328
Fax: (852)-3442-0522
Email: eddiema@cityu.edu.hk

Content List

Experimental Section

Physical measurements and instrumentation: ^{1}H NMR spectra were recorded by a Bruker AVANCE III system 400 MHz NMR spectrometer. Electrospray (ESI) mass spectra were measured by a Perkin-Elmer SCIEX API 365 LC/MS/MS system. Elementary analyses were performed on a Vario EL elementary analyzer. UV/Vis spectra were measured on a Hewlett Packard 8452A UV/Vis diode array spectrophotometer. Infrared spectra in the range 500 – 4000 cm^{-1} in KBr plates were recorded on a Perkin-Elmer Model FTIR-1600 spectrometer. Emission spectra were recorded by a SPEX FluoroLog 3-TCSPC spectrofluorimeter with a slit width of 5 nm and an integration time of 0.5 s. Emission lifetime measurements were carried out either with the SPEX FluoroLog 3-TCSPC, equipped with a N-370 NanoLED as the excitation source under the Fast MCS mode, or by a Spectra Physics nitrogen laser (excitation wavelength = 337 nm) at a maximum power of 15 mW. In the latter case, luminescence from samples was dispersed by a monochromator and was detected using a cooled Hamamastu R636-10 photon-multiplier in combination with a lock-in amplifier system. Decay spectra were monitored by a Hewlett Packard 54522A, 500 MHz oscilloscope. Emission quantum yields were measured by the method of Demas and Crosby with $[Ru(bpy)_3](PF_6)_2$ in degassed acetonitrile as standard (Φ_r = 0.062).[1] Sample and standard solutions were degassed with at least three freeze–pump–thaw cycles. For two-photon experiments, the 750 nm pump source was from the fundamental of a femtosecond mode-locked Ti:Sapphire laser system (output beam was of ca. 150 fs in duration with a repetition rate of 1 kHz). The lasers were focused to spot size of ca. 50 μm via an f = 10 cm lens onto the sample. The emitting light was collected with a backscattering configuration into a 0.5 m spectrograph and detected by a liquid nitrogen-cooled CCD detector. A power meter was used to monitor the uniform excitation. For two photon absorption cross-section

measurements, the theoretical framework and experimental protocol outlined by Webb and Xu [2] was adopted. The two-photon excitation (TPE) ratios of the reference and sample systems were given by Equation 1:

$$(1) \qquad \frac{\sigma_2^S \cdot \phi^S}{\sigma_2^R \cdot \phi^R} = \frac{C_R \cdot n_S \cdot F^S(\lambda)}{C_S \cdot n_R \cdot F^R(\lambda)}$$

where ϕ is the quantum yield, C is the concentration, n is the refractive index, and $F(\lambda)$ is the integrated photoluminescent spectrum. In our measurements, we have ensured that the excitation flux and the excitation wavelengths are the same for both the sample and the reference. The two-photon absorption cross-sections σ_2 of the cycloplatinated complexes were determined using Rhodamine 6G as a reference.[3, 4]

Crystal Structure Determination: Crystallographic data for complex **2**·$(ClO_4)_2$ are tabulated in Table S1 & S2 in the Supporting Information. All intensity data were collected on a Bruker Axs SMART 1000 CCD area detector using graphite-monochromated Mo-Kα radiation (λ = 0.71073 Å). All collected frames were processed with the software SAINT [5] and absorption correct was applied (SADABS)[6] to the collected reflections. The structure of the complex was solved by direct methods (SHELXTL)[7] in conjunction with standard difference Fourier syntheses. All non-hydrogen atoms were assigned with anisotropic displacement parameters. The hydrogen atoms were generated in their idealized positions and allowed to ride on the respective carbon atoms.

Materials and General Procedures: All starting materials, 2,6-dibromopyridine, *n*-butyl lithium (2.5 M in hexane), *N,N*-dimethylformamide, *N,N*-dimethylacetamide, phenylboronic acid, aqueous glyoxal (40%), aqueous NH_3 (30%), bromine, hydrobromic acid in acetic acid (33%), formamide, *bis*(diphenylphosphino)methane (dppm), triethylamine, and K_2PtCl_4 were purchased from Sigma-Aldrich and were used as received unless stated otherwise. Solvents used for synthesis were of analytical grade. Diethyl ether was distilled from sodium-benzophenone

and acetonitrile was distilled from anhydrous calcium hydride prior to use. Acetonitrile for photophysical measurements was distilled over potassium permanganate and calcium hydride. The synthesis of the cyclometalated ligand 2-(1*H*-imidazol-2-yl)-6-phenylpyridine (H***L*** $_1$) and 2-(1*H*-imidazol-4-yl)-6-phenylpyridine (H***L*** $_2$), and their cycloplatinated complexes [Pt(***L*** $_1$)Cl], [Pt(***L*** $_1$)(PPh_3)]$^+$, [Pt(***L*** $_2$)Cl] and [Pt(***L*** $_2$)(PPh_3)]$^+$ has already been reported in a previous publication.[8]

{[Pt(*L*$_1$)]$_2$(μ-dppm)}(ClO_4)$_2$ 1·(ClO_4)$_2$. To an acetonitrile solution (50 ml) of [Pt(***L*** $_1$)Cl] (0.1 g, 0.4 mmol) was added dppm (0.0426 g, 0.2 mmol). The mixture was stirred at room temperature for 12 h. A greenish-yellow suspension was obtained and a methanolic solution of $LiClO_4$ (0.43 g, 4 mmol) was added. The mixture was stirred at room temperature for another 12 h and the resulting clear yellow solution was filtered and evaporated to ca. 2 ml in volume. The desired product was precipitated by the addition of diethyl ether as a bright greenish-yellow solid. The product was collected by filtration, washed with diethyl ether and recrystallized by slow vapor diffusion of diethyl ether into its acetonitrile solution (0.11 g, 71 % yield). ESI-MS: 1216 $(M+1)^+$. ^{1}H NMR (400MHz, DMSO-d_6): δ 14.41 – 13.98 (br, 2H), 8.35 – 7.98 (br, 4H), 8.01 – 7.97 (t, J = 8.0 Hz, 2H), 7.93 – 7.68 (br, 2H), 7.65 – 7.59 (d, J = 8.0 Hz, 2H), 7.53 – 7.44 (m, 14H), 7.25 – 7.15 (d, J = 8.0 Hz, 2H), 7.10 – 6.90 (br, 2H), 6.71 – 6.67 (t, J = 8.0 Hz, 2H), 6.53 – 6.11 (br, 4H), 5.29 – 4.82 (br, 2H), 4.66 – 4.19 (br, 2H). Elemental analysis calcd (%) for $C_{53}H_{42}Cl_2N_6O_8P_2Pt_2$·2MeOH : C 44.69%, H 3.41%, N 5.69%. Found: C 44.45%, H 3.37%, N 5.71%

{[Pt(*L*$_2$)]$_2$(μ-dppm)}(ClO_4)$_2$ 2·(ClO_4)$_2$ was synthesized using the same method as complex **1**, with the use of [Pt(***L*** $_2$)Cl] as starting material (yield: 73%). ESI-MS: 1214 $(M - 1)^+$. ^{1}H NMR (400 MHz, DMSO-d_6): δ 12.90 – 12.65 (br, 2H), 8.51 – 8.20 (br, 4H), 7.92 – 7.88 (t, J = 8.0 Hz,

2H), 7.83 – 7.65 (br, 6H), 7.61 – 7.40 (br, 14 H), 7.38 – 7.36 (d, 2 H), 7.22 – 7.20 (d, J = 8.0 Hz, 2 H), 6.80 – 6.77 (t, J =7.4 Hz, 2H), 6.71 – 6.60 (br, 2H), 6.54 – 6.46 (t, J = 6.6 Hz, 2H), 5.15 – 4.95 (br, 2H), 4.51 – 4.38 (br, 2H). Elemental analysis calcd (%) for $C_{53}H_{42}Cl_2N_6O_8P_2Pt_2 \cdot 1H_2O$: C 44.45%, H 3.10%, N 5.87%. Found: C 44.60%, H 3.17%, N 5.82%.

Cell and acute brain slice cultures: HeLa cells were cultured in Dulbecco's Modified Eagle Medium (DMEM) supplemented with 10% foetal bovine serum (FBS), and 1% penicillin and streptomycin.

Dissociated dorsal root ganglion (DRG) cultures were prepared from postnatal day 1 C57BL/6 mice as previously described.[9] Briefly, DRGs were dissected out and mildly digested in collagenase and dispase II solution. Cells were trypsinized and dissociated mechanically using three flame-polished Pasteur pipette with different diameters. 3,000 DRG neurons were plated onto a poly-D-lysine (Sigma-Aldrich) and laminin-coated (Invitrogen) 35mm glass-bottomed petri dish (MatTek) containing Full Neurobasal (NB) medium (Gibco) supplemented with B27, 200 mM L-glutamine, penicillin/streptomycin, 50ng/ml NGF (Gibco), 2ng/ml GDNF and 10μM Ara-C (Sigma-Aldrich). All cells were kept in a humidified chamber with 5% CO_2 at 37 °C.

Acute brain slices were prepared from postnatal day 1 C57BL/6 mice. The slices were cut into 200 μm-thick using a vibrating blade microtome (Leica VT-1000 S) in artificial cerebrospinal fluid (ACSF; composition in mM: 138 NaCl, 3.5 KCl, 21 $NaHCO_3$, 0.6 NaH_2PO_4, 10 D-glucose, 1 $CaCl_2$, 3 $MgCl_2$).

MTT cell viability assay: HeLa cells were plated in triplicates into 96-well tissue culture plates. After 24 h, cells were treated with complex **1** at concentrations of 0, 1, 5.5 and 10 μM with 5% DMSO for 24 h. After that, the cells were incubated with 0.5 mg/ml of 3-(4,5-dimethylthiazol-2-

yl)-2,5-diphenyltetrazolium bromide (MTT) for 1 h before the addition of 10% Triton-X 100 in acidic isopropanol (0.1 M HCl). They were further incubated for 1 h for the dissolution of blue crystals formed. Finally, absorption was measured at 570 nm by using a microplate reader (PowerWave XS, BioTek). Relative viability was calculated by comparing absorbance of cells with and without the complex.

Microscopy: HeLa cells were grown on a glass-bottomed dish (MatTek) and maintained with CO_2 independent medium (Gibco), supplemented with 10% FBS. DRG neurons were grown in Full NB medium as described above for 17 h. After 17 h, the medium was replaced with CO_2 independent medium for fluorescent imaging. Acute brain slices were kept in ACSF for 2 h and transferred to a glass-bottomed dish (MatTek) just before fluorescent microscopy. All the cell and tissue cultures were maintained at 37 °C by using a CO_2 microscope cage incubation system (Okolab) during fluorescent microscopy.

For single-photon microscopy, images were either obtained by a Carl Zeiss Axioplan 2 fluorescent microscope using a UV light source, or a Leica TCS SP5 spectral confocal microscope equipped with a diode laser. Specimens were imaged by using either an Argon laser with excitation wavelength of 458 nm (for complex **1**) or a HeNe laser with excitation wavelength of 543 nm (for LysoTracker Red) through an ACS APO 40× NA 1.15 objective. Average laser power of 40% and gain level of 900V were used in image acquisition. Detection bandwidth was ranged from 500-600 nm (for complex **1**) or 600-700 nm (for LysoTracker Red).

For multi-photon microscopy, images were collected by a Leica TCS SP5 spectral confocal microscope equipped with a Ti:sapphire laser. An excitation wavelength of 750 nm, a HCX PL APO CS 40× NA 1.25 (for HeLa cells), or an HCX PL APO CS 63× NA 1.30 (for both DRG neuron and acute brain slice culture) objective, average multi-photon power of 2310W and gain

level of 900V were used in image acquisition. Detection bandwidth was ranged from 500-650 nm.

All confocal images of HeLa cells were obtained using the same scanning parameters including the scan speed (400Hz), scanning mode (*xyz*), line averaging (2), frame averaging (3) and resolution (512×512 pixels).

Time-lapse images were obtained with 1 sec (primary DRG neurons) or 0.7 sec (acute brain slice) intervals. 120 to 200 frames of images were collected from each series of time-lapse imaging using *xyt* mode at 600 Hz scan speed.

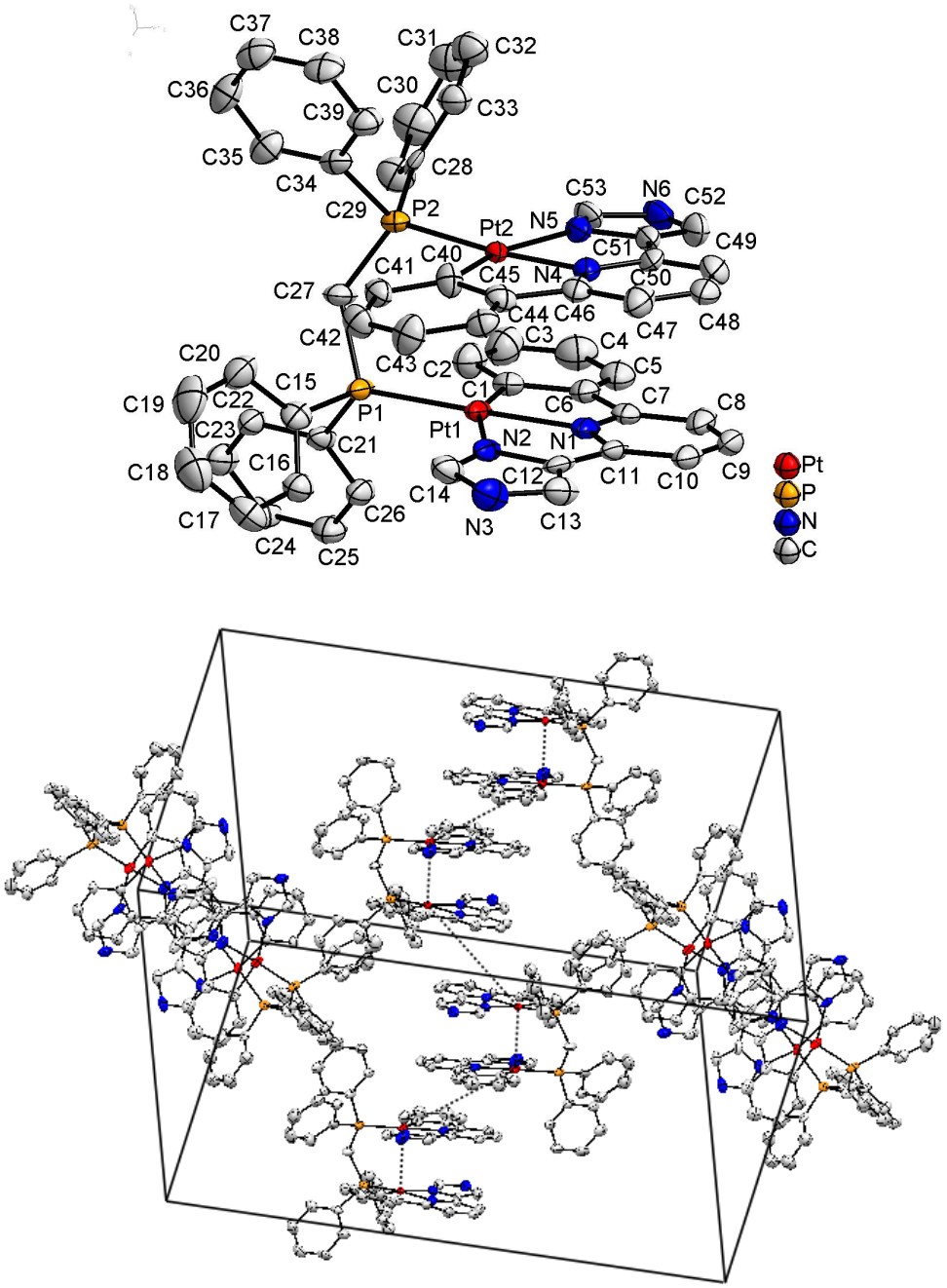

Fig. S1 Molecular structure and crystal packing of **2** with the numbering scheme adopted.

Thermal ellipsoids are shown at the 50% probability level.

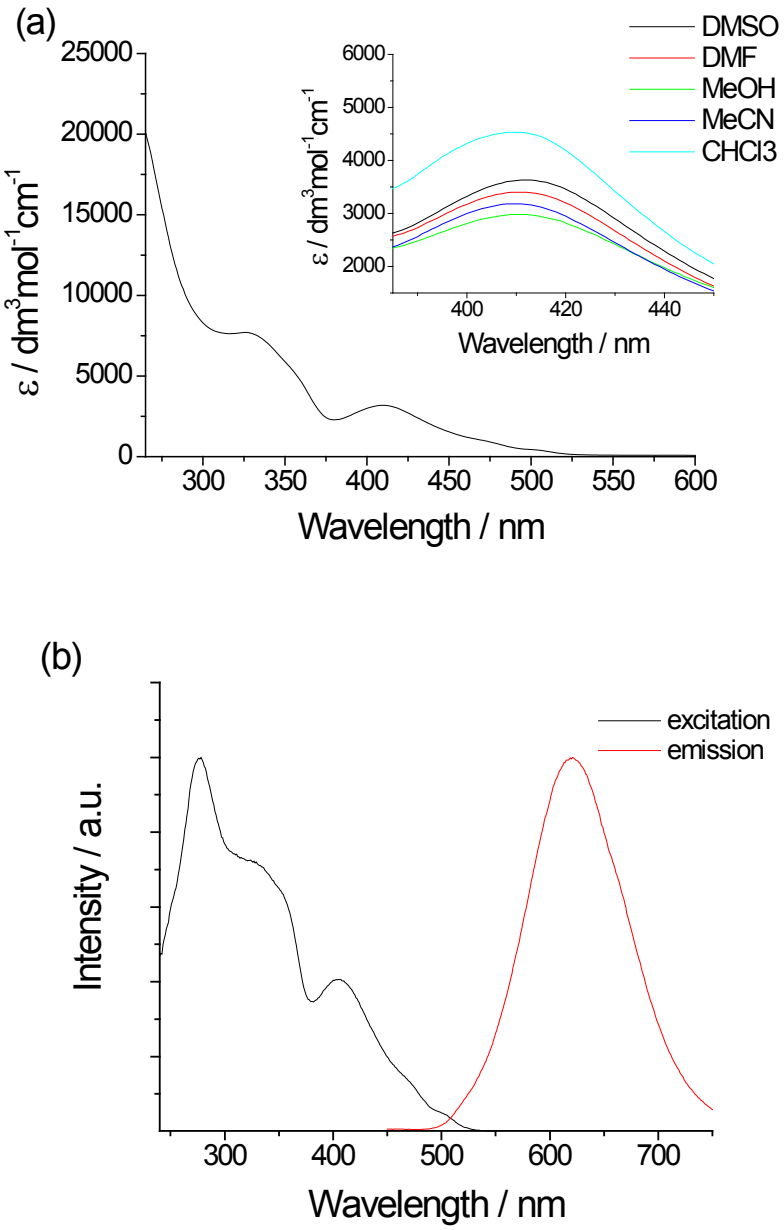

Fig. S2 Spectroscopic properties of $\{[Pt(\boldsymbol{L_1})]_2(\mu\text{-dppm})\}(ClO_4)_2$ **1**·$(ClO_4)_2$ in acetonitrile at 298 K: (a) UV-vis absorption spectra, with solvent dependence of the absorption band at 385 – 450 nm shown in the inset; (b) normalized excitation and emission spectra (concentration = 5×10^{-5} M).

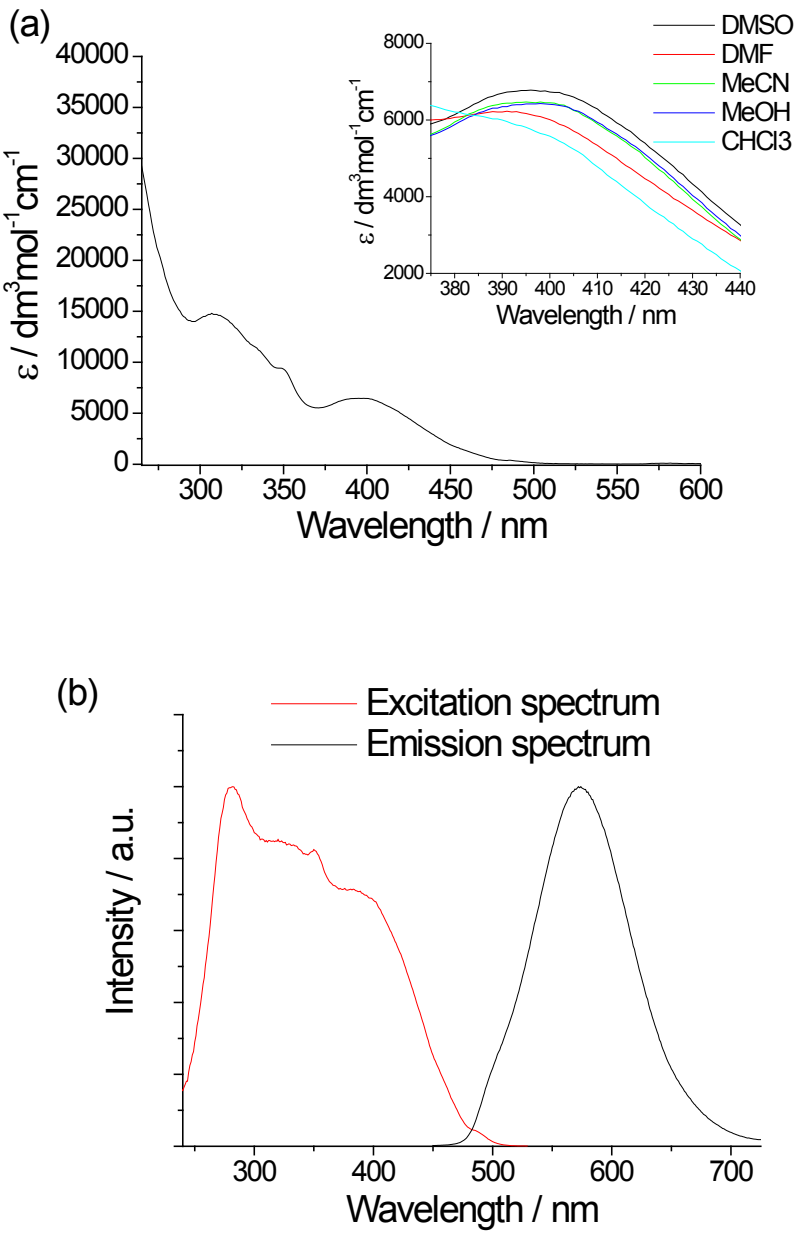

Fig. S3 Spectroscopic properties of $\{[Pt(\boldsymbol{L_2})]_2(\mu\text{-dppm})\}(ClO_4)_2$ **2**·$(ClO_4)_2$ in acetonitrile at 298 K: (a) UV-vis absorption spectra, with solvent dependence of the absorption band at 375 – 440 nm shown in the inset; (b) normalized excitation and emission spectra (concentration = 5×10^{-5} M).

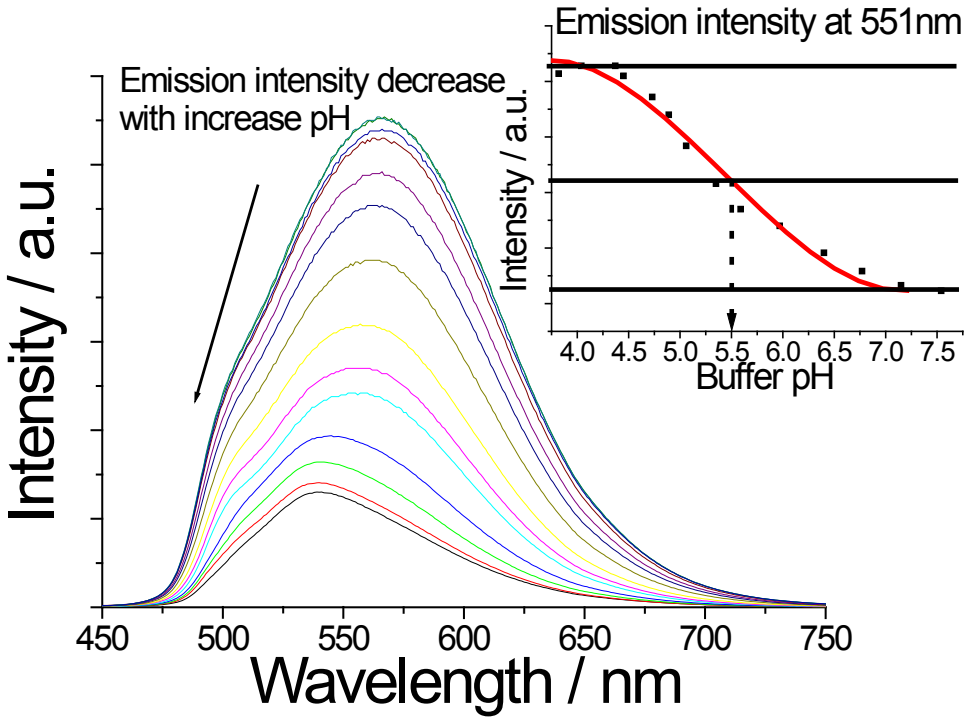

Fig. S4 Luminescent responses of $\{[Pt(\boldsymbol{L_2})]_2(\mu\text{-dppm})\}(ClO_4)_2$ **2**·$(ClO_4)_2$ in 2:1 (v/v) DMF / aqueous buffer (5×10^{-5} M) to changes in media pH at 298 K. (Excitation λ = 355 nm)

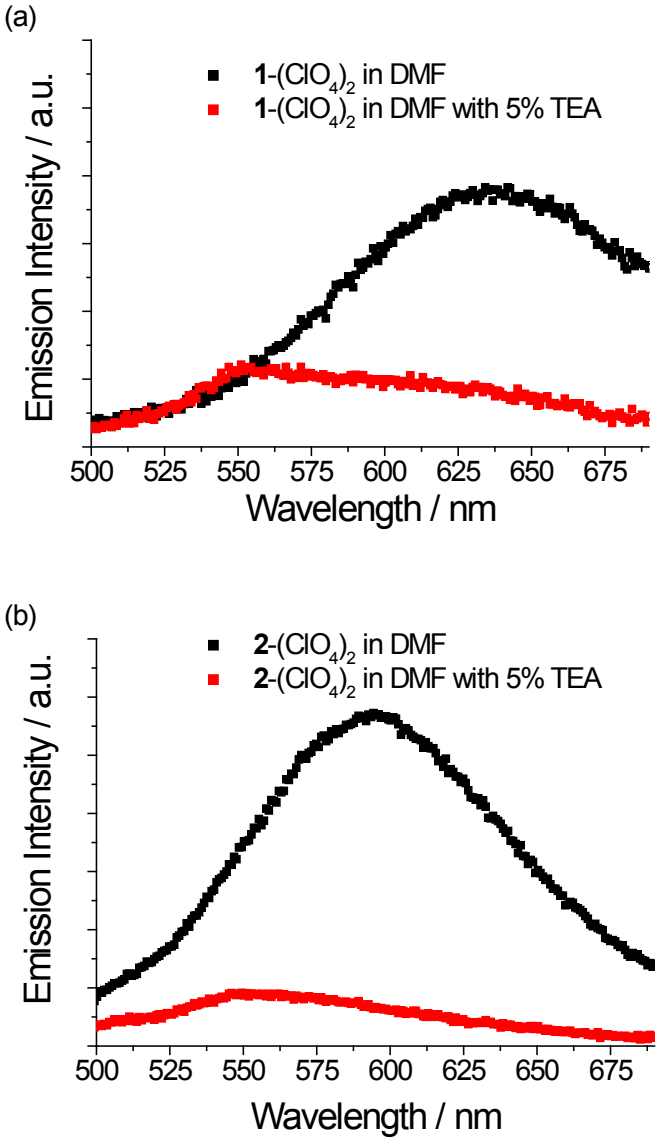

Fig. S5 Two-photon induced luminescent spectra of complex **1** (a) and **2** (b), both at 5×10^{-4} M, in DMF at 298 K with and without the addition of 5% triethylamine for the deprotonation of the imidazolyl-*NH* on the cyclometalating ligands. (λ_{ex} = 750 nm)

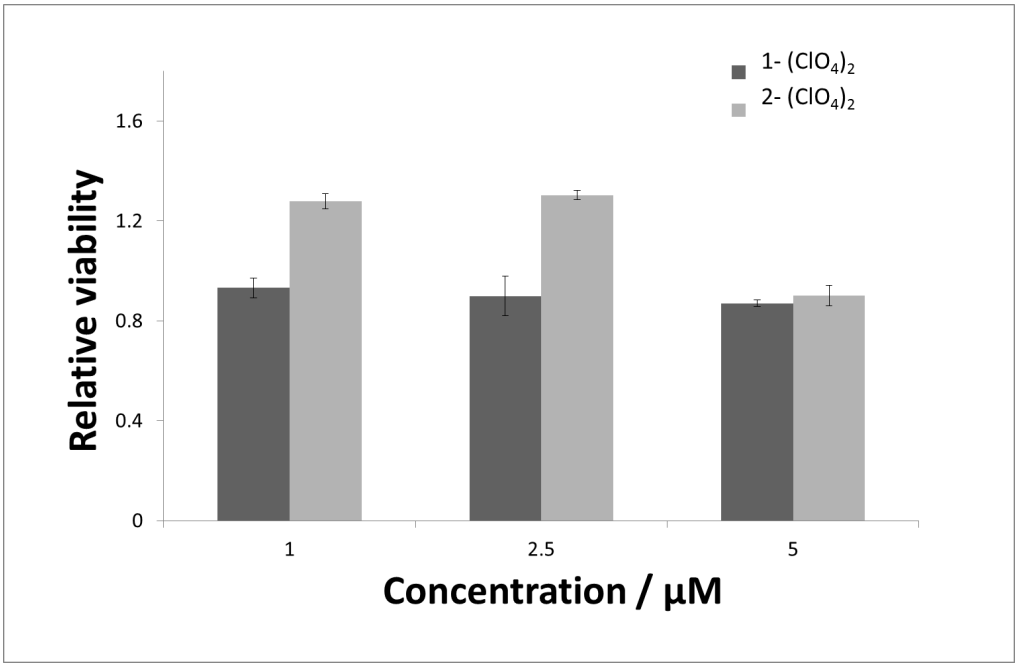

Fig. S6 MTT assays of cytotoxicity of complexes **1** & **2** on HeLa cells with 2 h exposure.

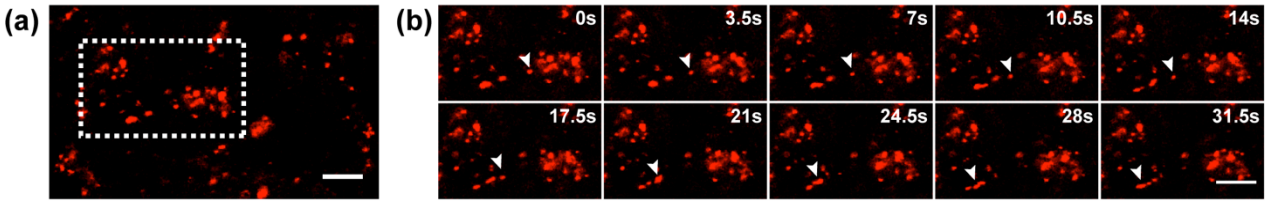

Fig. S7 Two-photon microscopy images of acute brain slice after 2 h exposure to 5 μM of complex **1**: (a) Image (λ_{ex} = 750 nm) of acute brain slice stained with complex **1**. Lysosomes were localized inside the cell bodies and axons. (b) Time-lapse images from the white box in (a) showed the vesicle trafficking along the axons of brain tissue. White arrowheads indicated the movement of lysosomes. Scale bar: 10 μm.

Table S1 Selected bond lengths (Å) and angles (deg) of complex **2**.

{[Pt(***L*****2**)]$_2$(μ-dppm)}$(ClO_4)_2$ **2**·$(ClO_4)_2$			
Pt(1) – C(1)	2.035(9)	Pt(2) – C(40)	2.043(11)
Pt(1) – N(1)	2.027(6)	Pt(2) – N(4)	2.019(9)
Pt(1) – N(2)	2.128(7)	Pt(2) – N(5)	2.114(9)
Pt(1) – P(1)	2.237(19)	Pt(2) – P(2)	2.245(3)
Pt(1) – Pt(2)	3.135 (2)		
C(1)-Pt(1)-N(1)	80.78(3)	N4 Pt2 C40	81.34(4)
N1 Pt1 N2	78.15(3)	N4 Pt2 N5	78.05(4)
C1 Pt1 N2	158.78(3)	C40 Pt2 N5	159.39(4)

Table S2 Crystal data and structure refinement details of complex **2**.

	2
Empirical formula	$C_{55}\ H_{50}\ Cl_2\ N_6\ O_{10}\ P_2\ Pt_2$
Colour	Yellow
Formula weight	1478.03
Temperature, K	133(2)
Wavelength, Å	1.54178
Crystal system	Monoclinic
Space group	C 1 2/c 1 (15)
a, Å	21.4316(10)
b, Å	18.6779(8)
c, Å	28.2587(11)
α, deg	90.00
β, deg	92.868(4)
γ, deg	90.00
Volume, $Å^3$	11297.71(84)
Z	8
Density (calculated), g cm^{-3}	1.73782
Absorption coefficient, mm^{-1}	11.053
F(000)	5776
Crystal dimensions, mm	-
θ range for data collection, deg	3.33 to 24.99
Limiting indices	$-10 \leq h \leq 10$, $-18 \leq k \leq 18$, $-12 \leq l \leq 12$
Reflections collected	10015
Independent reflections (R_{int})	22322 (0.0237)
Completeness to θ = 25.00º, %	99.6
Observed reflections [I > 2α(I)]	9606
Max. and min. transmission	-
Data / restraints / parameters	9606 / 586 / 959
Goodness-of-fit on F2	1.259
Final R indices [I > 2 α(I)]	R1 = 0.0511 wR2 = 0.1035
R indices (all data)	R1 = 0.0530 wR2 = 0.1043
Largest different peak and hole, $eÅ^{-3}$	1.821 and -1.482

Table S3 Summary of photophysical properties of the cycloplatinated complexes **1** & **2**.

Complex	Emission in fluid solution (at 298K)			
	λ_{max} / nm [a]	τ_o / μs [b]	Φ_{lum} [c]	TPA Cross Section / GM [d]
{[Pt(***L*** $_1$)]$_2$(μ-dppm)}$(ClO_4)_2$ **1**·$(ClO_4)_2$	621	2.06	0.19	56
{[Pt(***L*** $_2$)]$_2$(μ-dppm)}$(ClO_4)_2$ **2**·$(ClO_4)_2$	574	2.10	0.21	35

[a,b] Measured in acetonitrile (5×10^{-5} M), with excitation λ at 355 nm.

[c] Using $[Ru(bpy)_3](PF_6)_2$ in degassed acetonitrile at 298K ($\phi_r = 0.062$) as reference.

[d] Using Rhodamine 6G as reference.

References

1. J. N. Demas and G. A. Crosby, *Journal of Physical Chemistry*, 1971, 75, 991-&.

2. C. Xu and W. W. Webb, *Journal of the Optical Society of America B-Optical Physics*, 1996, 13, 481-491.

3. M. Albota, D. Beljonne, J. L. Bredas, J. E. Ehrlich, J. Y. Fu, A. A. Heikal, S. E. Hess, T. Kogej, M. D. Levin, S. R. Marder, D. McCord-Maughon, J. W. Perry, H. Rockel, M. Rumi, C. Subramaniam, W. W. Webb, X. L. Wu and C. Xu, *Science*, 1998, 281, 1653-1656.

4. T. Kohl, K. G. Heinze, R. Kuhlemann, A. Koltermann and P. Schwille, *Proceedings of the National Academy of Sciences of the United States of America*, 2002, 99, 12161-12166.

5. *SAINT*, Siemens Energy and Automation, Madison, WI, 1994 - 1996.

6. G. M. Sheldrick, *SADABS, Empirical Absorption Correction Program*, University of Göttingen, Germany, 1997.

7. G. M. Sheldrick, *SHELXTLTM Reference Manual, version 5.1*, Siemens Energy and Automation, Madison, WI, 1997.

8. Y. M. Ho, C. K. Koo, K. L. Wong, H. K. Kong, C. T. L. Chan, W. M. Kwok, C. F. Chow, M. H. W. Lam and W. Y. Wong, *Dalton Transactions*, 2012, 41, 1792-1800.

9. C. H. Ma, T. Omura, E. J. Cobos, A. Latremoliere, N. Ghasemlou, G. J. Brenner, E. van Veen, L. Barrett, T. Sawada, F. Gao, G. Coppola, F. Gertler, M. Costigan, D. Geschwind and C. J. Woolf, *J Clin Invest*, 2011, 121, 4332-4347.